DESIGN MODEL FOR COMPOSITE BEAM TO REINFORCED CONCRETE WALL JOINTS

José Henriques; Luís Simões da Silva
ISISE - Department of Civil Engineering, University of Coimbra, Portugal
jagh@dec.uc.pt; *luisss@dec.uc.pt*

Isabel Valente
ISISE - Department of Civil Engineering, Engineering School, University of Minho, Portugal
isabelv@civil.uminho.pt

ABSTRACT

In this paper, a design model for composite beam to reinforced concrete wall joints is presented and discussed. The proposed model is an extension of the component method to this type of joints. The characterization of the active components is therefore performed in terms of force-deformation curves. In this type of joints, special attention is paid to the steel-concrete connection where “new” components, not covered in EN1993-1-8, are activated. The application of the model allows obtaining the joint properties in terms of moment-rotation curve. The accuracy of the proposed model is verified by comparison against available experimental and numerical results. The latter were developed in the FE program ABAQUS and previously validated against experimental results.

1. INTRODUCTION

In many office and car park type of buildings there is the need to combine reinforced concrete structural walls with steel and/or composite members. In such structural systems the design of the joints is a challenge due to the absence of a global approach. Designers are faced with a problem that requires knowledge in reinforced concrete, anchorage in concrete and steel/composite behaviour. Because of the different design philosophies, especially in what regards the joints, no unified approach is currently available in the Eurocodes.

The component method is a consensual approach for the design of steel and composite joints with proven efficiency. Therefore, in this paper, a design model extending the scope of the component method to steel-to-concrete beam-to-wall joints is proposed. To address the problem, a composite beam to reinforced concrete wall joint, experimentally tested within the RFCS research project “InFaSo” [1], was chosen. The joint configuration under analysis was developed to provide a semi-continuous solution, allowing transfer of bending moment between the supported and supporting members. The joint depicted in Figure 1 may be divided in two zones: i) upper zone, connection between the reinforced concrete slab and the wall; ii) bottom zone, connection between the steel beam and the reinforced concrete wall. In the upper zone, the connection is achieved by extending and anchoring the longitudinal reinforcement bars of the slab (*a*) into the wall. Slab and wall are expected to be concreted in separate stages and therefore, the connection between these members is only provided by the longitudinal reinforcement bars. In the bottom zone, fastening technology is used to connect the steel beam to the reinforced concrete wall.

Thus, a steel plate (*b*) is anchored to the reinforced concrete wall using headed anchors (*c*), pre-installation system. The plate is embedded in the concrete wall with aligned external surfaces. Then, on the external face of the plate, a steel bracket (*d*) is welded. A second plate (e) is also welded to this steel bracket however, not aligned in order to create a “nose”. The steel beam with an extended end plate (*f*) sits on the steel bracket, and the extended part of the end plate and steel bracket “nose” achieve an interlocked connection avoiding the slippage of the steel beam out of the steel bracket. A contact plate (*g*) is placed between the beam end plate and the anchor plate, at the level of the beam bottom flange.

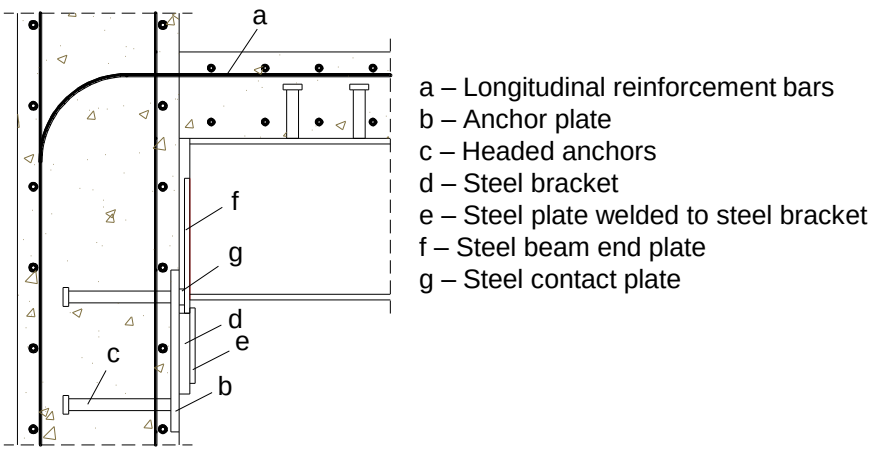

Figure 1: Composite beam to reinforced concrete wall joint configuration studied in [1]

According to the structural demands, the joint configuration can cover a wide range of combination of design loads (M-V-N) without modifying significantly the connection between the steel and the concrete parts. The versatility of the joint is illustrated in Figure 2. Three working situations are possible: i) semi-continuous with medium/high capacity to hogging bending moment, shear and axial compression; ii) pinned for high shear and axial compression; iii) pinned for high shear and axial tension. According to the detailing of Figure 1, because of the weakness of the “nose” system, the sagging bending moment capacity is very limited and strongly dependent of the “nose” resistance. For the same reason, the resistance to tensile loading is also reduced. Therefore, the application to cyclic loading, such as seismic action, is restricted. Pinned behaviour of the joint is very easily obtained by removing the connection between the slab and the wall. Consequently, in terms of erection, this is a very efficient solution; however, for the above reasons, the joint should not be subject to axial tension. Whenever this is a requirement, adding a fin plate as shown in Figure 2 (iii) provides a straightforward solution. In this case, the tension capacity is improved and due to the symmetry of the joint, cyclic loading may be applied. In the present paper only the semi-continuous joint solution subject to hogging bending moment is analysed.

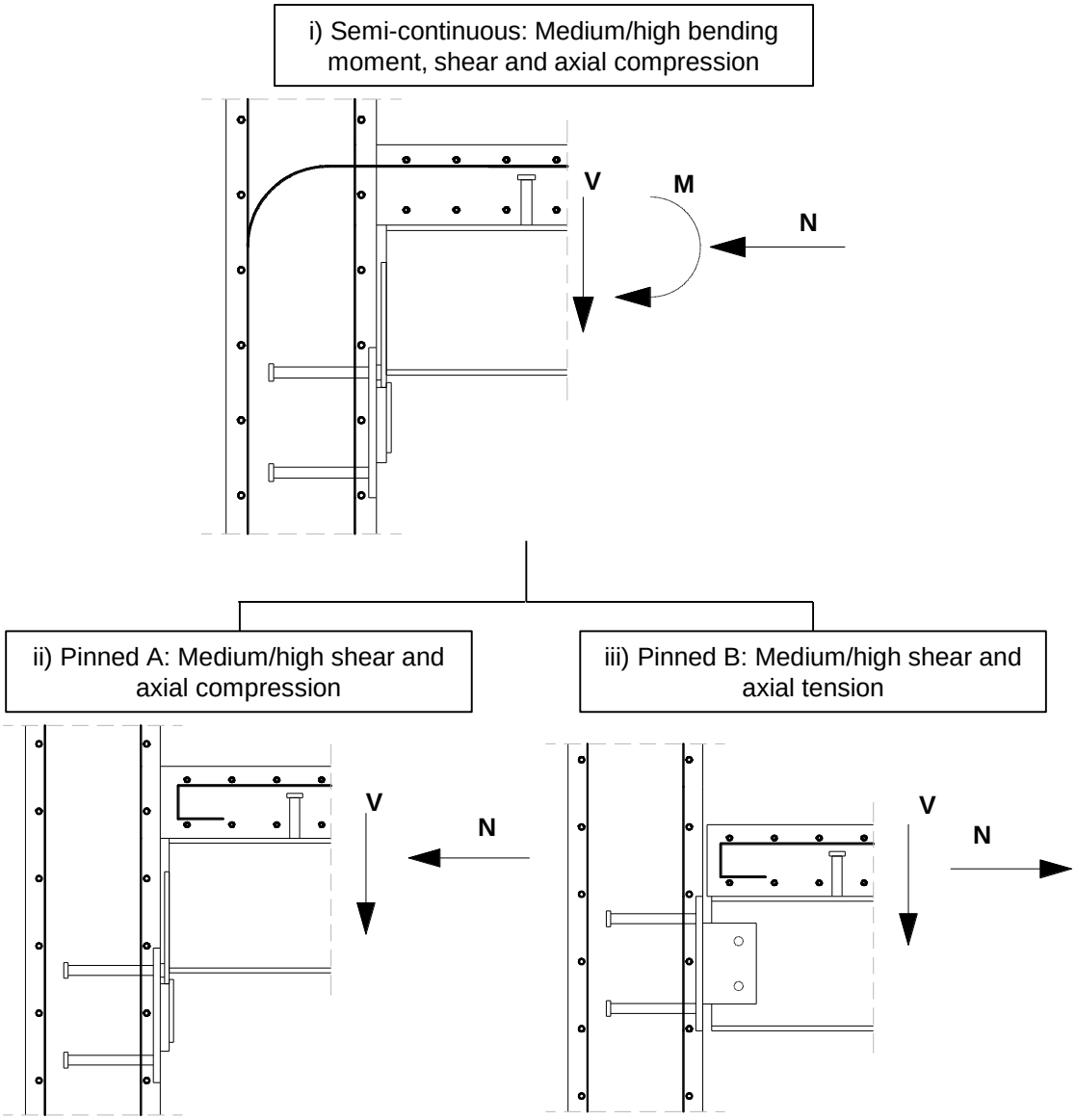

Figure 2: Versatility of the steel-to-concrete joint for different loading conditions

2. SOURCES OF JOINT DEFORMABILITY AND JOINT MODEL

To understand the behaviour of the joint under bending moment and shear force the mechanics of the joint is identified. The assumed stress flows are schematically represented in Figure 3. Accordingly, in the upper zone, only tension is transferred through the longitudinal reinforcement. Also, in this region, there is no shear and no tension is assumed to be transferred through the concrete, from the slab to the wall, as the small bond developed is neglected. In the bottom zone, the shear load is transferred from the steel beam to the reinforced concrete wall according to the following path: a) from the beam end-plate to the steel bracket through contact pressure; b) from the anchor plate to the reinforced concrete wall through friction, between the plate and the concrete and between the shaft of the headed anchors and the concrete through bearing. Also in the bottom zone, compression is transferred to the reinforced concrete wall through the contact plate between the beam end-plate and the anchor plate. Then, in the reinforced concrete wall the high tension and compression loads introduced by the joint flow to supports.

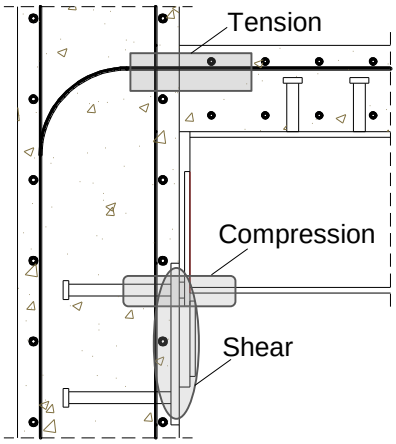

Figure 3: Stress flow on the semi-continuous joint under bending moment and shear loading

According to the described stress flows, corresponding to hogging bending moment, the active components are identified and listed in Table 1 and their location is shown in Figure 4-a). Note that the number attributed to the joint components is set for the present paper and disregards the usual numbering proposed in [2]. Components 7, 8, 9 and 10 should not control the behaviour of the joint as their activation only results from the out-of-plane deformation of the bottom and top edges of the anchor plate in compression at the level of the upper anchor row. Due to the presence of an anchor row at the bottom part, this should act similarly to a prying force and consequently, the anchor row is activated in tension. In what respects to component 11, denominated as “Joint Link”, it represents the equilibrium of stresses in the reinforced concrete wall zone adjacent to the joint.

According to the identified components, a representative spring and rigid link model is illustrated in Figure 4-b). Three groups of springs are separated by two vertical rigid bars. The rigid bars avoid the interplay between tension and compression components, simplifying the joint assembly. Another simplification is introduced by considering a single spring to represent the joint link. In what concerns the tension springs, it is assumed that slip and the longitudinal reinforcement are at the same level although slip is observed at the steel beam – concrete slab interface. In this model, at the bottom part of the joint, rotational springs (5) are considered in the anchor plate to represent the bending of this plate. In a simplified model, the behaviour of these rotational springs, as well as the effect of the bottom anchor row, should be incorporated into an equivalent translational spring representing the contribution of the anchor plate to the joint response. Each group of components is discussed in the next chapter.

Table 1: List of active components in the composite beam to reinforced concrete wall joint subject to hogging bending moment

Component ID	Basic joint component	Type/Zone
1	Longitudinal steel reinforcement in slab	Tension
2	Slip of composite beam	Tension
3	Beam web and flange	Compression
4	Steel contact plate	Compression
5	Anchor plate in bending under compression	Bending/Compression
6	Concrete	Compression
7	Headed anchor in tension	Tension
8	Concrete cone	Tension
9	Pull-out of anchor	Tension
10	Anchor plate in bending under tension	Bending/Tension
11	Joint Panel	Tension and Compression

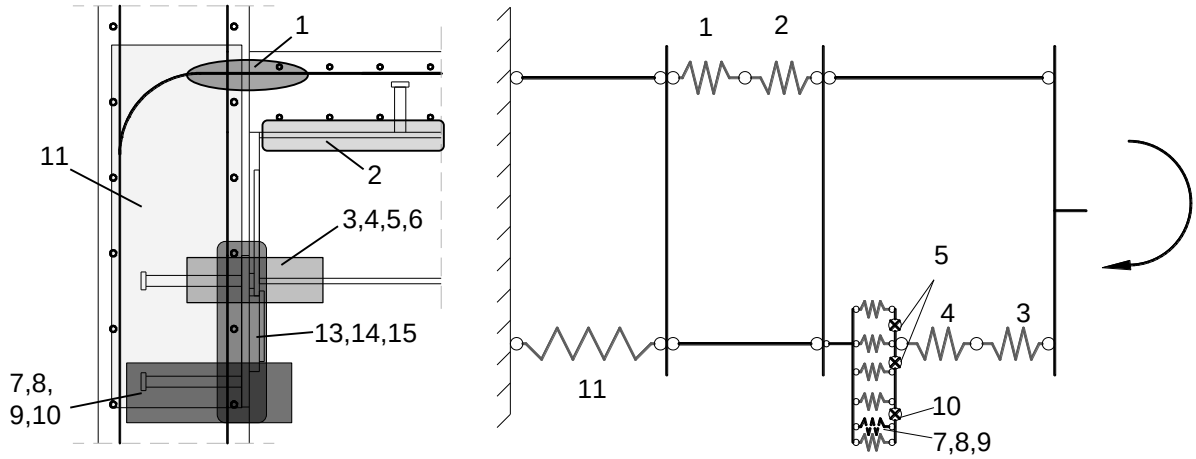

a) Location of the joint components identified

b) Joint component model

Figure 4: Application of the component method to a composite beam to reinforced concrete wall joint subject to hogging bending moment

3. CHARACTERIZATION OF ACTIVATED JOINT COMPONENTS

3.1 Components in tension zone

In case full interaction is achieved between the slab and the steel beam, the longitudinal reinforcement in tension limits the resistance of the tension zone of the joint. This component is common in composite joints where the longitudinal reinforcement is continuous within the joint or its anchorage is assured. In EN 1994-1-1[3], each layer of longitudinal reinforcement is considered as an additional bolt row contributing to the resistance of the joint. The longitudinal reinforcement within the effective width of the concrete slab is assumed to be stressed up to its yield strength. In terms of deformation, a stiffness coefficient is provided by the code which takes into account: i) the configuration of the joint, double or single sided; ii) the depth of the column; iii) the area of longitudinal reinforcement within the effective width of the concrete flange; iv) the loading on the right and left side, balanced or unbalanced bending moment. No guidance is provided to estimate the deformation capacity. Sufficient deformation capacity to allow a plastic distribution of forces should be available if the ductility class of the reinforcement bars is B or C, according to EN 1992-1-1[4]. A more sophisticated model of this component can be found in [5] where the

behaviour of the longitudinal reinforcement is modelled taking into account the embedment in concrete and the resistance goes up to the ultimate strength of steel. The component is modelled by means of a multi-linear force-displacement curve with hardening. This model allows to estimate the deformation at ultimate resistance. This deformation is then assumed as the deformation capacity of the component. Table 2 summarizes the analytical expressions for both models. Figure 5 illustrates the force-deformation curves characterizing the behaviour of the components according to these models. In the ECCS [5] model, the initial range is very stiff as the concrete is uncracked. Then, as cracks form in the concrete a loss of stiffness is noticed until there is stabilization in cracking. At this stage, the response of the longitudinal reinforcement bar recovers the proportionality between stress and strain of the bare steel bar up to the yield strength. Finally, the ultimate resistance is achieved assuming that the bars may be stressed up to their ultimate strength. In the Eurocode model, linear elastic behaviour is considered up to the yielding of the longitudinal reinforcement bar.

Table 2: Analytical expressions for longitudinal reinforcement component

Reference		Expressions
EN 1994-1-1 [3]	Resistance	$F_{sy} = \sigma_y A_{sr}$
	Stiffness coefficient	$k_{sr} = \frac{A_{sr}}{3{,}6h}$
	Deformation capacity	Not given
ECCS Publication Nº109 [5]	Resistance	$F_s = \sigma_{sr,i} A_{sr}$ With $\sigma_{sr1} = \frac{f_{ctm} k_c}{\rho}\left[1 + \rho \frac{E_s}{E_c}\right]$ $\sigma_{srn} = 1{,}3\sigma_{sr1}$
	Deformation	$\Delta \leq \Delta_{sry}$: $\Delta = \varepsilon(h + L_t)$ $\varepsilon_{sr1} = \frac{\sigma_{sr1}}{E_s} - \Delta\varepsilon_{sr}$ $\Delta\epsilon_{sr} = \frac{f_{ctm} k_c}{E_s \rho}$ $\rho < 0{,}8\%$: $\Delta_{sru} = 2L_t \varepsilon_{srmu}$ $\rho \geq 0{,}8\%\ and\ a < L_t$: $\Delta_{sru} = (h + L_t)\varepsilon_{srmu}$ $\rho \geq 0{,}8\%\ and\ a > L_t$: $\Delta_{sru} = (h + L_t)\varepsilon_{srmu} + (a - L_t)\varepsilon_{srmy}$

In this joint, the composite beam is designed to have full interaction between the steel beam and the RC slab; therefore, no limitation to the joint resistance is expected from component 2: slip of composite beam. In what concerns the deformation of this component, as verified in [6], a small contribution to the joint rotation may be observed. According to [7], the slip at the connection depends on the nearest stud to the wall face. Under increasing load this stud provides resistance to slip until it be-

comes plastic. Additional load is then assumed to be resisted by the next stud deforming elastically until its plastic resistance is reached. Further load is then carried by the next stud and so forth. The deformation capacity of the component is then limited by the deformation capacity of the shear connection between the concrete slab and the steel beam. In EN 1994-1-1 [3], the contribution of the slip of the composite beam is taken into account by multiplying the stiffness coefficient of the longitudinal steel reinforcement in tension by a slip factor (k_{slip}).

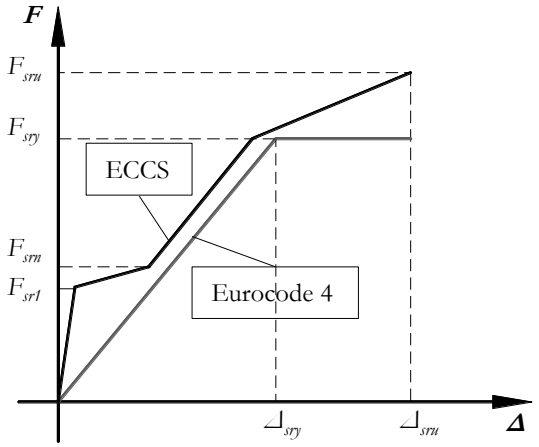

Figure 5: Behaviour of the component longitudinal steel reinforcement bar in tension

3.2 Components in the compression zone

In the compression zone, the beam web and flange in compression and the steel contact in compression are components already covered by EN1993-1-8 [2] and EN 1994-1-1 [3]. Furthermore, according to the scope of the experimental tests [1], their contribution to the joint response was limited to the elastic range. In this way, for the characterization of these components, reference is given to [2] and [3].

In what concerns the anchor plate in compression, this connection introduces into the problem the anchorage in concrete. Because the main loading is compression, the anchorage is not fully exploited. In order to reproduce its behaviour, a sophisticated model of the anchor plate in compression is under development. As illustrated in Figure 4, several components are activated carrying tension, compression and bending loading. Due to the similarities of the problem, the model under development is a adapted version of the Guisse *et al.* [8] for column bases. In the absence of specific tests on the anchor plate in compression, the model is based on numerical investigations. Figure 6 depicts the idealized mechanical model and the reference numerical model. The steel-concrete contact is reproduced by considering a series of extensional springs that can only be activated in compression. Because of the deformation of the anchor plate, the anchor row on the unloaded side is activated in tension and increases anchor plate in compression resistance and stiffness. For the anchor row on the unloaded side, a single extensional spring concentrates the response of three components: i) anchor shaft in tension; ii) concrete cone failure; iii) headed anchor pull-out failure. Then, three rotational springs are considered to reproduce the bending of the plate according to its deformation. The location of these springs is based on the numerical observations (see Figure 6-b). The properties of these components are given in Table 3. For the involved parameters please check the references given in the table.

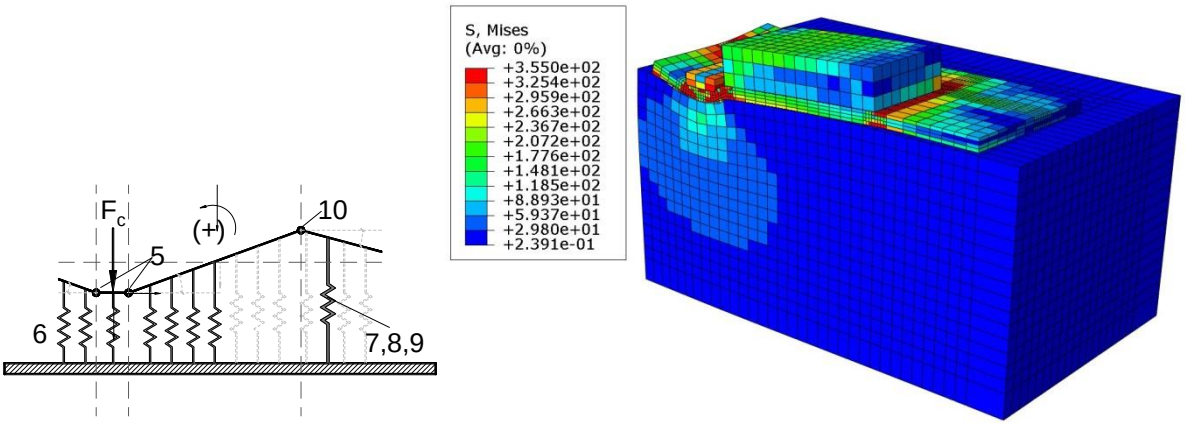

a) Idealized mechanical model b) Reference numerical model

Figure 6: Anchor plate connection

Table 3: Analytical characterization of the components relevant for the anchor plate in compression

Component		Reference	
6	Resistance	Guisse*et al.*[8]	$F_i = \left[\frac{f_j - E_c\varepsilon_{c2}}{\varepsilon_{c2}^2}\left(\frac{\delta_i}{h_{c,eq}}\right)^2 + E_c\left(\frac{\delta_i}{h_{c,eq}}\right)\right]A_{c,i}$
	Deformation		$\delta_i = \varepsilon_i h_{c,eq}$
7	Resistance	EN 1993-1-8[2]	$N_{st} = n\left(\frac{\pi d^2}{4}\right)f_y$
	Deformation		$\delta_{st,y} = \frac{N_{st}}{k_{st}}$ with $k_{st} = \frac{E_a\left(\frac{\pi d^2}{4}\right)}{h_{ef}}$
8	Resistance	CEN-TS[9]	$N_c = \left(\frac{A_{c,N}}{A_{c,N}^0}\right)\psi_m N_c^0$ With $N_c^0 = 16.8\sqrt{0.95 f_{ck,cube}}h_{ef}^{1.5}$
	Deformation	-	rigid
9	Resistance	CEN-TS[9]	$N_{PO} = 11 f_{ck}\frac{\pi(d_h^2 - d^2)}{4}$
	Deformation	Furche[10]	$\delta_{PO} = \alpha_p \frac{k_a k_A}{C_1}\left(\frac{N}{A_h 0.95 f_{ck,cube} n}\right)^2$
5 and 10	Resistance	Conventional	$M_y = f_y\frac{b_{ap}t_{ap}^2}{6}$ $M_{pl} = f_y\frac{b_{ap}t_{ap}^2}{4}$
	Deformation		$\Phi_u = \frac{2 \times 0.15}{t_{ap}}$

Figure 7 shows the comparison between the results of the numerical and the analytical model. These are given in terms of load applied on the anchor plate and deformation in the direction of the load at the point of application of the load. Despite the excellent accuracy of the analytical model, its full validity is yet to be established,

as a parametric study has shown some deviations between the models. The improvement of the model is currently under development.

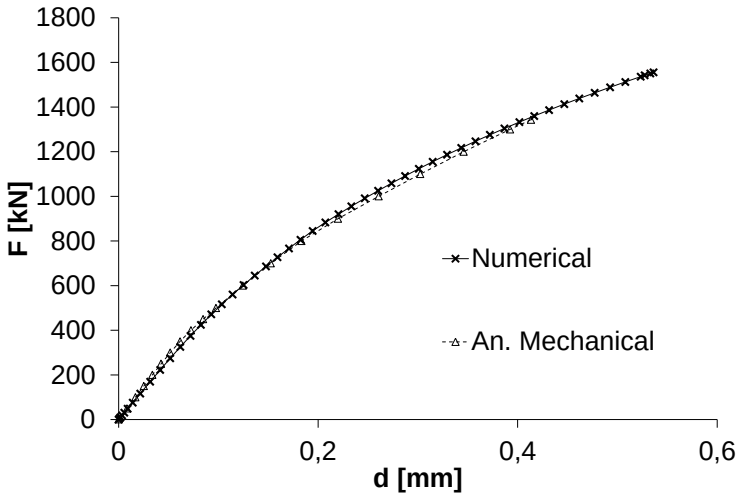

Figure 7: Comparison of results between analytical and numerical model

The above model aims to accurately reproduce the behaviour of the anchor plate in compression. However, it is perhaps too complex for design purposes. Thus, a simplified modelling of the anchor plate in compression is envisaged. Again because of the similarities of the problem, a modified version of the T-stub in compression [2] is foreseen as follows:

- For resistance and stiffness, the β factor is set equal to 1, as the use of grout between plate and concrete is not expected.
- For stiffness, an exact value of the bearing width c has been determined according to [11] instead of the approximation given in the EN 1993-1-8 [2]. Thus, c is taken equal to 1,46t instead of 1,25t.

Consequently, components 5 to 10 are replaced in the joint component model, shown in Figure 4, by a single equivalent spring representing the T-stub in compression. This is the model used later in section 4.

3.3 Joint Link

The joint link is a component to consider the resistance and deformation of the reinforced concrete wall in the zone adjacent to the joint. The loading on this member coming from the above part of the structure may affect this component. However, only the joint loading is considered in the present study. As for the anchor plate under compression, no specific experimental tests have been performed to analyse this part of the joint. Therefore, a simplified analysis is being performed numerically. Because of the nature of this part of the joint, reinforced concrete, the model is based on the strut-and-tie method commonly implemented in the analysis of reinforced concrete joints. The problem is 3D, increasing its complexity, as the tension load is introduced with a larger width than the compression, which may be assumed concentrated within an equivalent dimension of the anchor plate (equivalent rigid plate as considered in T-stub in compression). Thus, a numerical model considering only the reinforced concrete wall and an elastic response of the material has been tested to identify the flow of principal stresses. These show that compression stress-

es flow from the hook of the longitudinal reinforcement bar to the anchor plate. In this way the strut-and-tie model (STM) depicted in Figure 8-a) is idealized. Subsequently, in order to contemplate the evaluation of the deformation of the joint, a diagonal spring is idealized to model the diagonal compression concrete strut, as illustrated in Figure 8-b). The ties correspond to the longitudinal steel reinforcement bars already considered in the joint model. The properties of this diagonal spring are determined as follows.

- Resistance is obtained based on the strut and nodes dimension and admissible stresses within these elements. The node at the anchor plate is within a tri-axial state. Therefore, high stresses are attained (confinement effect). In what concerns the strut, because of the 3D nature, stresses tend to spread between nodes. Giving the dimensions of the wall (infinite width), the strut dimensions should not be critical to the joint. Thus, the node at the hook of the bar is assumed to define the capacity of the diagonal spring. The resistance of the spring is then obtained according to the dimensions of this node and to the admissible stresses in the node and in the strut. For the latter, the numerical model indicates the presence of transverse tension stresses which have to be taken into consideration. The admissible stresses are defined according to EN 1992-1-1 [4].
- The deformation of the diagonal spring is obtained as follows. A non-linear stress-strain relation for the concrete under compression, as defined in [4], is assumed. The maximum stress is given by the limiting admissible stress as referred above. Then, deformation is calculated in function of the length of the diagonal strut and the concrete strain.

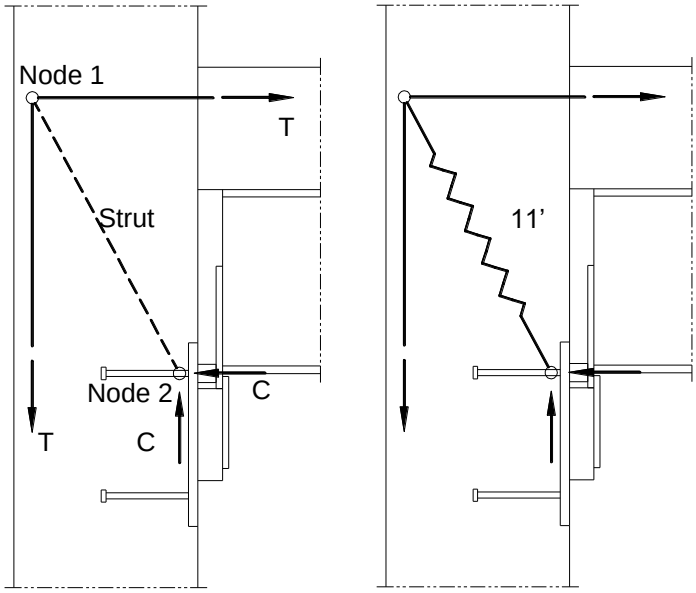

a) STM b) Single diagonal spring
Figure 8:Joint link modelling

Table 4 gives the admissible stresses for nodes and struts according to EN 1992-1-1 [4]. Node 1, illustrated in Figure 9, is characterized by the hook longitudinal reinforcement bar. The represented dimension is assumed as defined in the CEB Model Code [12]. In what concerns the width of the node, based on the numerical observations, it is considered to be limited by the distance between the external longitudinal reinforcement bars within the effective width of the slab. The numerical

model demonstrates that the longitudinal reinforcement bars are sufficiently close, as no relevant discontinuity in the stress field is observed. Though, this is an issue under further investigation and depending on the spacing of the reinforcing bars, this assumption may or may not be correct.

Table 4: Admissible stresses in STM elements according to EN 1992-1-1[4]

Element	Admissible stresses
Node 1	$0{,}75vf_{cd}$
Node 2	$3vf_{cd}$
Strut	$0{,}6vf_{cd}$ with $v = 1 - f_{ck}/250$

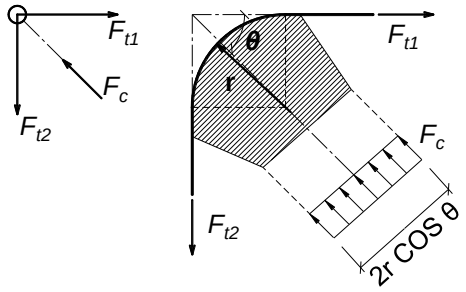

Figure 9: Definition of the dimension related to the hook of the longitudinal reinforcement bar in Node 1, according to the CEB Model Code [12]

Finally, to simplify the assembling of the joint model, the diagonal spring representing the joint link component is converted in a horizontal spring as represented in Figure 4. The properties of the horizontal spring are directly obtained from the diagonal spring determined as a function of the angle of the diagonal spring.

4. APPLICATION OF THE DESIGN MODEL TO A COMPOSITE BEAM TO REINFORCED CONCRETE WALL JOINT

In order to obtain the joint properties, the assembly of the model depicted in Figure 4 is performed, simplified by the use of a modified version of the T-stub in compression model, as described in section 3. The assembly procedure is then direct, no distribution of resistance is required amongst rows, as only one tension row is identified. In order to determine the joint bending moment and rotation, it is required to define the lever arm h_r of the joint. According to the joint configuration, it is assumed that the lever arm is the distance between the centroid of the longitudinal steel reinforcement and the mid thickness of bottom flange of the steel beam. Thus, the smallest resistance of the activated components governs the bending moment resistance and may be expressed as follows.

$$M_j = Min(F_i)h_r \quad (1)$$

F_i represents the resistance of all activated components within the joint under bending moment loading determined as described above.

In what respects the joint rotation, the contribution of all components should be considered. Again, as only one tension and one compression row is activated, the

joint rotation can easily be obtained. The component governing the resistance controls the rotation capacity of the joint. The joint rotation capacity may be determined as follows.

$$\Delta_u = \frac{\sum_1^n \Delta_i}{h_r} \quad (2)$$

$\Sigma\Delta_i$ represents the sum of the deformation of the activated components for a load level equal to the resistance of the governing component. In the case of the governing component, all its deformation capacity should be considered.

The accuracy of the described model has been assessed using the experimental results performed at the University of Stuttgart within the RFCS research project InFaSo [1]. The tested specimens consisted of a cantilever composite beam supported by a reinforced concrete wall. The joint configuration depicted in Figure 1 was used to connect both members. A vertical load was applied at the free edge of the composite beam up to failure. The load induced in the joint a hogging bending moment. The geometrical and material properties, as well as detailed discussion of the tests, may be found in [13].

In Figure 10, the moment-rotation curves for two of the tested specimens are compared. The results of a numerical model are also included. The calibration and validation of this numerical model is presented in [14]. The parameter varied between the selected specimens is the diameter of the longitudinal reinforcement bars (percentage of reinforcement within the slab): Test 1 – 6xΦ16; Test 2 – 6xΦ12. In what concerns the analytical model, the ECCS [5] model for the longitudinal steel reinforcement was considered. For the slip of the composite beam, the approach proposed in [7] is used. The curves show a good approximation between analytical, numerical, and experimental results. The accuracy of the analytical and numerical approaches in relation to the experimental results are quantified in Table 5. In terms of resistance the approximation is excellent. In terms of rotation at maximum bending moment, the results of the analytical approach are interesting taking into account that this parameter usually is not quantified. The resistance of each component according to the analytical model is given in Table 6. The percentage of resistance activated of each component is also included. It can be observed that as in the experimental tests, the longitudinal reinforcement bar in tension is the governing component. According to the analytical estimation, in Test 1, the beam web and column in compression is close to its full activation. On the other hand, in both tests, the steel contact plate and the anchor plate in compression are the components with lowest level of activation in comparison to their load capacity.

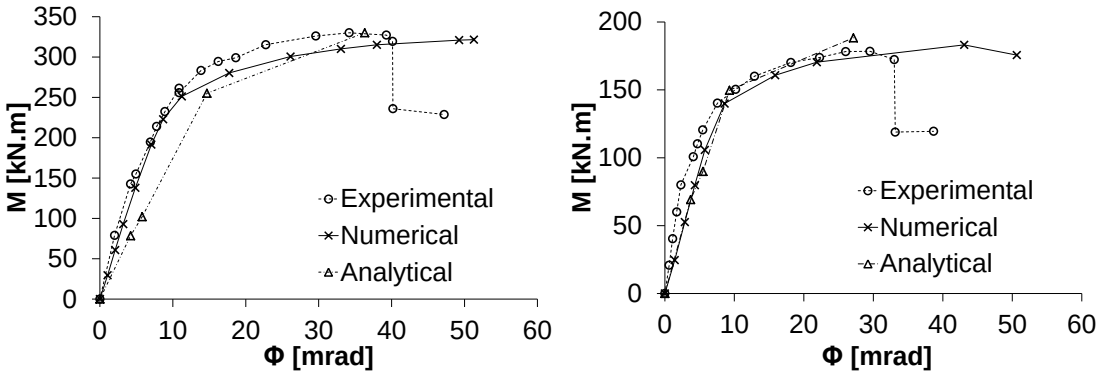

a) Test 1 b) Test 2

Figure 10: Moment-rotation curves comparing experimental, numerical and analytical results

Table 5: Summary of the global results of the joint properties and quantification of the approximation to experimental results

Approach	Test	$M_j/M_{j,test}$	$\Phi_j/\Phi_{j,test}$	$S_j/S_{j,test}$
Analytical	1	0,99	0,90	0,85
	2	1,05	0,92	0,87
Numerical	1	0,97	1,27	1,10
	2	1,02	1,46	0,88

Table 6: Resistance of the components according to analytical model and % of activation

Components	Test 1		Test 2	
	Fr,i [kN]	% Active	Fr,i [kN]	% Active
1	811,9	100,0	460,9	100,0
2	1200,0	67,7	1200,0	38,4
3	824,9	98,4	824,9	55,9
4	2562,0	31,7	2562,0	18,0
5 to 10	2017,6	40,2	2017,6	22,8
11	1224,8	66,3	930,0	49,6
Governing	*Component 1*		*Component 1*	

5. CONCLUSIONS AND GENERAL RECOMMENDATIONS

In this paper, a design model based on the component method for composite beam to reinforced concrete wall is proposed and compared with experimental and numerical results. Although some of the approaches of the individual components are incomplete, at the current stage, the model demonstrates to be accurate. Based on the presented results and considerations achieved during this research work, some design suggestions are proposed:

i) Designing the longitudinal reinforcement in the composite beam to be the governing component allows a better control of the joint response. The characterization of this component can be more accurate in an inelastic range in comparison with the other activated components. Furthermore, if the steel reinforcement bars are class C (according to [4]) a ductile response can be obtained.

ii) Due to the complexity of the problem, reducing the Joint Link component to a single spring is a simplification with practical interests. However, this approach is limited and therefore, the failure of the joint in this component should be avoided.

REFERENCES

[1] Kuhlmann, U., Eligehausen, R., Wald, F., da Silva, L., Hofmann, J. "New market chances for steel structures by innovative fastening solutions", Final report of the RFCS project INFASO, project Nº RFSPR-CT-2007-00051, Brussels, 2012.

[2] European Committee for Standardization – CEN. EN 1993-1-8. Eurocode 3: Design of steel structures. Part 1-8: Design of joints, Brussels, 2005.

[3] European Committee for Standardization – CEN. EN 1994-1-1. Eurocode 4: Design of composite steel and concrete structures. Part 1-1: General rules and rules for buildings, Brussels, 2004.

[4] European Committee for Standardization – CEN. EN 1992-1-1. Eurocode 2: Design of concrete structures. Part 1-1: General rules and rules for buildings, Brussels, 2004.

[5] European Convention for Constructional Steelwork – ECCS. Design of Composite Joints for Buildings. ECCS Publication nº109, Technical Committee 11, Composite Structures, First Edition, Belgium, 1999.

[6] Aribert, J. M. "Influence of Slip on Joint Behaviour", Connections in Steel Structures III, Behaviour, Strength and Design, Third International Workshop, Trento, Italy, May 29-31, 1995.

[7] Anderson, D.; Najafi, A. A. "Performance of Composite Connections: Major Axis End Plate Joints", Journal of Constructional Steel Research, vol. 31, pp. 31-57, 1994.

[8] Guisse, S, Vandegans, D, Jaspart, J-P. Application of the component method to column bases: Experimentation and development of a mechanical model for characterization. Research Centre of the Belgian Metalworking Industry, MT195, Liège, 1996.

[9] European Committee for Standardization – CEN. CEN/TS 1992-4: Design of fastenings for use in concrete, Final Draft, Brussels, 2009.

[10] Furche, J. ZumTrag- und Verschiebungsverhalten von Kopfbolzenbeizentrischem Zug. PhD Thesis (in German), University of Stuttgart, Stuttgart, 1994.

[11] Steenhuis M, Wald F, Sokol Z, Stark J. Concrete in compression and base plate in bending. Heron 2008; Vol. 53 No. 1/2; 51-68.

[12] Comité Euro-International du Béton - CEB. CEB-FIP Model Code 1990 : Design Code. Lausanne, 1993.

[13] Henriques J, Ozbolt A, Žižka J, Kuhlmann U, Simões da Silva L, Wald F. Behaviour of steel-to-concrete joints II: Moment resisting joint of a composite beam to reinforced concrete wall. Steel Construction Design and Research (Ed. Ernst &Sohn), Volume 4, August 2011 Nº3, 161-165.

[14] Henriques, J, Simões da Silva, L, Valente, I. Numerical modeling of composite beam to reinforced concrete wall joint: mechanical behavior and 3D interactions. Computers & Structures, 2012 (Submitted).